Acta Biomaterialia 192 (2025) 119–127

Contents lists available at ScienceDirect

Acta Biomaterialia

journal homepage: www.elsevier.com/locate/actbio

Full length article

Electro-deformation spectroscopy: A unified method for simultaneous electrical and mechanical characterization of single cells

E Du [a,b,*], Hongyuan Xu [a], Liliana Ponkratova [a]

[a] Department of Ocean and Mechanical Engineering, College of Engineering and Computer Science, Florida Atlantic University, Boca Raton, FL 33431, United States
[b] Department of Biomedical Engineering, College of Engineering and Computer Science, Florida Atlantic University, Boca Raton, FL, United States

ARTICLE INFO

Keywords:
Electro-deformation spectroscopy
Electrical properties
Mechanical properties
Red blood cells
Microfluidics
Single-cell assay

ABSTRACT

The intrinsic electrical and mechanical properties of cells are not only valuable biophysical markers reflective of physiological conditions but also play important roles in the development and progression of human diseases. Existing single-cell techniques are restricted to assessing either mechanical or electrical properties. We introduce the development of electro-deformation spectroscopy (EDS), namely the frequency-dependent electro-deformation, as a new method for simultaneous electrical and mechanical characterization of individual cells in suspension. To facilitate the practical use of this technology, we developed a testing procedure that evaluates red blood cells (RBCs) directly from whole blood in a simple microfluidic system, employing an electric field magnitude of 34 kV/m over a frequency range of 15 MHz to 100 kHz. The EDS measurement is performed under stationary conditions without special cell stabilization, at a moderate throughput of 50–100 cells per minute. We develop an experimental-computational framework to decouple cell electromechanics by optimizing the most suitable parameters of the relative permittivity of cell membrane, cytoplasm electrical conductivity, and membrane shear modulus. This technique, tested on RBCs from 4 healthy human samples, revealed membrane relative permittivity of 3.6 – 5.8, membrane shear modulus of 2.2 – 2.8 μN/m, and cytoplasm conductivity of 0.47 – 0.81 S/m. EDS analysis identifies the marked intrasample heterogeneity and individual variability in both cellular electrical and mechanical properties. The EDS framework can be readily used to test RBCs across different species, pathological states, and other cell types of similar structures as RBCs.

Statement of significance: This work introduces electro-deformation spectroscopy (EDS) as a unified method for simultaneous electrical and mechanical characterization of single cells in suspension. This is the first-of-its-kind technology for such purposes. EDS can be performed in a simple microfluidic system with minimal sample preparation, making it a convenient and powerful tool for label-free, non-invasive single-cell analysis. We validate the applicability of EDS by measuring the intrasample heterogeneity and individual variability based on the electromechanical parameters of interest for human red blood cells. Single-cell EDS has the potential to enable rapid and reliable detection of cellular changes by diseases or drug treatments and provide insights into the fundamental bioelectromechanical mechanisms of cellular adaptation and dysfunction. This work advances the field of single-cell analysis and contributes to the development of biomaterials and biotechnologies based on cellular electromechanics.

1. Introduction

Cellular electrical parameters, such as equivalent cell resistance, membrane capacitance and cytoplasm conductivity, are tied to cellular biophysical attributes and activities associated with cell size, growth, proliferation, and fusion [1,2]. Cellular mechanical properties, such as deformability, membrane shear modulus, viscosity, and fatigue are indicative of their structural integrity and dynamics of the cytoskeleton and plasma membrane; and importantly, cell mechanics influence mechanotransduction pathways [3] and regulate metabolic activities in a reciprocal manner [4]. Research on the cell biomechanics and biophysics and their subcellular components have significantly advanced our understanding on how cellular properties affect, and are affected by, the development and progression of human diseases such as

* Corresponding author at: Department of Ocean and Mechanical Engineering, College of Engineering and Computer Science, Florida Atlantic University, Boca Raton, FL 33431, United States.
E-mail address: edu@fau.edu (E. Du).

https://doi.org/10.1016/j.actbio.2024.12.012
Received 25 July 2024; Received in revised form 26 November 2024; Accepted 3 December 2024
Available online 5 December 2024

blood infectious diseases [5,6], cancer [7], and neurodegenerative diseases [8,9]. In addition, understanding single cell electrical and biomechanical properties has enabled development of novel methods for disease diagnostics and treatment monitoring [6,10–12].

Single-cell assay technologies are widely used in microfluidic systems, enabling precision detection of diseased cells and quantification of biological heterogeneity. Label-free, non-invasive techniques are especially valuable for assessing the intrinsic electrical and mechanical properties of single cells. Generally, these two types of cellular parameters are studied in isolation using different methods. On the one hand, cellular electrical properties or dielectric properties are measured using electrical technologies and alternating current (ac) electrokinetic methods. Electrical impedance spectroscopy (EIS, or dielectric spectroscopy) are conventional electrical techniques that study the response of a sample subjected to an applied electric field of fixed or varying frequencies of kilohertz (kHz) to gigahertz (GHz). EIS implemented into microfluidic systems for single cell analysis, known as electrical impedance flow cytometry, was demonstrated useful for high throughput measurements of single cells, such as membrane capacitance, cytoplasm conductivity, and dielectric properties of cytoplasm in health and diseases [13–15]. Alternative methods are ac electrokinetics, including dielectrophoresis (DEP) and electrorotation, which study the movement and rotation of single cells subjected to an applied electric field of fixed or varying frequencies of kHz – megahertz (MHz) [16–18]. Theory and applications of these electrical and ac electrokinetic methods for single cell analysis are reviewed in detail in recent literature [19–21]. On the other hand, mechanical properties of single cells, such as elasticity and shear modulus, are assessed based on their response to applied external forces or force fields. Various techniques exist for single-cell mechanical measurement, such as atomic force microscopy (AFM), optical tweezers, micropipette aspiration, and magnetic twisting cytometry, as reviewed in detail in recent papers [6,22,23]. Many of these techniques, such as optical tweezers and micropipette aspiration, have been used as standard tools for probing subcellular regions in single cells, ranging from primary cells such as RBCs [24], cancer cells [25], to a variety of cell lines [26]. Recent development in optical tweezers has revealed the strain rate and temperature dependences of RBC mechanics [27]. A recent study showed throughput of optical tweezers was improved to be 4 cells per minute [28]. Overall, mechanical measurement of single cells is less efficient as compared to the electrical measurements in several aspects, such as throughput, complexity in setup, and automation [29].

Despite numerous prior studies on the mechanical and electrical characteristics of single cells, research that integrates both types of information remains scarce. Recent findings have revealed that alterations in cytoskeletal organization can affect cellular electrical conductivity, in addition to influencing cellular mechanical properties [30]. Another study reported on a microfluidic device for simultaneous mechanical and electrical characterization of single osteoblast cells [31]. Although the method it uses relies on delicate integration of two separate techniques, impedance spectroscopy and micropipette aspiration, into a microfluidic platform, the results demonstrated the potential of using both membrane mechanics and cytoplasm conductivity to achieve a comprehensive characterization of single cells.

To date, according to our knowledge, there is no unified technology capable of simultaneous measurements of electrical and mechanical properties of single cells. One potential method is electro-deformation (or electrodeformation, E-D), referring to the uniaxial elongation of cell membranes induced by applied electric fields at fixed frequencies. It has been widely used in measuring cell mechanical characteristics in microfluidic systems [32–35]. In addition to mechanical measurement, the frequency dependence in the E-D induced shape transition of phospholipid vesicles was examined [36]. Recently, we demonstrated that E-D modulated by amplitude-shift-keying technique is a useful tool to study the fatigue behavior of cells, namely the gradual mechanical degradation in cell membranes due to cyclic loading of shear stress [37] and cyclic hypoxia challenge [38]. Nevertheless, despite the cellular heterogeneity, calibration of the electrical forces for single cell mechanical characterization is conducted, assuming constant universal dielectric properties determined from other techniques. This may lead to error in force calibration and goes on to the elastic and shear modulus, while also overlooking the cellular heterogeneity [13].

In this paper, we introduce a new single-cell assay for assessing electrical and mechanical properties, termed electro-deformation spectroscopy (EDS), which relies on the principle of frequency-dependent electro-deformation of cells. EDS is conducted within a microfluidic system that employs electric fields (34 kV/m) over a frequency range from 15 MHz to 100 kHz. The frequency-dependent responses of RBCs from whole blood are measured in suspension. Using an experimental-computational framework, we analyze the elongation of individually tracked cells across various frequencies. Optimization approach using MATLAB *fmincon* function is used to find the most suitable parameters for the cell electro-deformation across the testing frequencies. The capability of the technique is demonstrated through measurements of the membrane permittivity, cytoplasm conductivity, and membrane shear modulus of single RBCs from four different human blood samples.

2. Materials and methods

2.1. Mathematical models of cell electromechanics

E-D occurs due to interfacial Maxwell–Wagner polarization across cellular membranes [39]. The induced surface charges across the cell membrane interact with the electric field, resulting in distributed forces [40] on the two cell halves and thus uniaxial elongation of cell membranes,

$$\langle \boldsymbol{F} \rangle = \oint_S \langle \boldsymbol{\sigma}^{\mathrm{MST}} \rangle \cdot \boldsymbol{n} dS \tag{1}$$

where S is the outer surface area of the cell model, and $\boldsymbol{n}$ is the unit vector normal to the cell surface. The time averaged Maxwell stress tensor (MST), $\langle \boldsymbol{\sigma}^{\mathrm{MST}} \rangle$ is determined by,

$$\langle \boldsymbol{\sigma}^{\mathrm{MST}} \rangle = \frac{1}{4} Re\ [\widetilde{\varepsilon}](\boldsymbol{E}\boldsymbol{E}^{*} + \boldsymbol{E}^{*}\boldsymbol{E} - |\boldsymbol{E}|^2 \boldsymbol{I} \tag{2}$$

where $\widetilde{\varepsilon}$ is the complex electrical permittivity, $\boldsymbol{E}$ the electrical field, $\boldsymbol{I}$ is the unit tensor.

E-D occurs in companion with positive dielectrophoresis (p-DEP), known as the movement of dielectric particle towards the higher field strength, due to a net force induced by the electric fields. Assuming a triaxial ellipsoid shape, the net electrical force is well described by the classical formula [41],

$$\langle \boldsymbol{F}_{DEP} \rangle = \frac{\pi}{4} abc \cdot \varepsilon_m \cdot Re(f_{CM}) \cdot \nabla \boldsymbol{E}_{rms}^2 \tag{3}$$

where a, b, and c are the diameters along x, y, and z axes. ε is the permittivity of the surrounding medium, and $\nabla \boldsymbol{E}_{rms}^2$ is the root-mean-square (rms) value of the gradient of electric field strength square.

$Re(f_{CM})$ is the real part of the Clausius Mossotti (CM) factor (f_{CM}). For a biological cell such as red blood cell, value of f_{CM} can be determined

from a single-shell structure (Fig. 1a), following a concentric multi-shell model [42,43],

$$f_{CM} = \frac{1}{3}\frac{\left(\varepsilon^*_{mem} - \varepsilon^*_m\right)\left[\varepsilon^*_{mem} + A_1\left(\varepsilon^*_{cyto} - \varepsilon^*_{mem}\right)\right] + \rho\left(\varepsilon^*_{cyto} - \varepsilon^*_{mem}\right)\left[\varepsilon^*_{mem} - A_1\left(\varepsilon^*_{mem} - \varepsilon^*_m\right)\right]}{\left(\varepsilon^*_m + A_1\left(\varepsilon^*_{mem} - \varepsilon^*_m\right)\right)\left[\varepsilon^*_{mem} + A_1\left(\varepsilon^*_{cyto} - \varepsilon^*_{mem}\right)\right] + \rho A_2(1 - A_2)\left(\varepsilon^*_{cyto} - \varepsilon^*_{mem}\right)\left(\varepsilon^*_{mem} - \varepsilon^*_m\right)} \tag{4}$$

where the subscripts cyto, mem and m stand for cytoplasm, membrane and medium, respectively. $E^* = \varepsilon - \frac{j\sigma}{\omega}$ with ω, ε and σ as the angular frequency, dielectric permittivity and conductivity, respectively. $\rho = \frac{(a-t)(b-t)(c-t)}{abc}$. $A_{i=1,2}$ is the depolarization factor, defined as

$$A_i = \frac{a_i b_i c_i}{2}\int_0^\infty \frac{d_s}{(s + a_i^2)B_i},\ i = 1,\ 2 \tag{5}$$

where $B_i = \sqrt{\left(s + a_i^2\right)\left(s + b_i^2\right)\left(s + c_i^2\right)}$, $a_1 = a$, $b_1 = b$, $c_1 = c$, $a_2 = a - t$, $b_2 = b - t$, $c_2 = c - t$, and t denotes the thickness of cell membrane, often a constant value, 4.5 nm.

The most rigorous method to determine the resultant electrical force responsible for E-D is to employ the MST as described in Eq. (1). This can be done numerically using finite element analysis, such as COMSOL Multiphysics. For the convenience of cell-specific force calibration, we develop an adaptive scheme, which approximates the MST force with point-force components exerted on the two far ends of the stretched cell, as used in our previous E-D study [44]. Briefly, the magnitude of the two equivalent point force components can be calculated using Eq. (3). It is noted that the value of ∇E^2_{rms} follows a power function of distance away from the electrode edge in the elongation axis,

$$\nabla E^2_{rms} = k \cdot d^{\zeta} \tag{6}$$

where d is the distance in μm, measured from the edge of electrode to the end point of the stretched cell. In the current study, the coefficients $k = C_V \times 1.245 \times 10^{15}$, $C_V = 0.5625$, and $\zeta = -0.86$, were computed using a 2-dimensional model by COMSOL Multiphysics 5.2 (COMSOL, Inc., Burlington, MA) based on the experimental conditions. For a typical microscopic particle, the two equivalent point forces can be one order of magnitude different due to the power function as described in Eq. (6). Thus, it is reasonable to approximate that a cell undergoing E-D is fixed on one end at the electrode edge while the other end is pulled by a point force (Fig. 1b) with the force magnitude computed by,

$$\langle F^* \rangle = \frac{\pi}{4} abc \cdot \varepsilon_m \cdot Re(f_{CM}) \cdot 7 \times 10^{14} \cdot d^{-0.86} \tag{7}$$

For simplicity, the value of d can be approximated by the major diameter, a of the stretched cell in the current study. In response to E-D excitation, cell membrane exhibits a time-dependent uniaxial deformation due to its inherent viscoelasticity. Particularly, membrane of red blood cells is highly resistant to dilation, deformation occurs at essentially constant element surface area [45]. The elongation and the in-plane uniaxial tension can be described by the first-order tension--deformation law, according to the Kelvin-Voigt solid model (Fig. 1b) [46,47],

$$T_s = \frac{\mu}{2}\left(\lambda^2 - \lambda^{-2}\right) \tag{8}$$

where T_s is the uniaxial tension, λ is the extension ratio, and μ is the membrane shear modulus of elasticity. In the case of E-D induced cell elongation observed at the equilibrium state, the corresponding shear stress is approximated by,

$$T_s = \frac{\langle F^* \rangle}{2b} \tag{9}$$

The induced shear strain is,

$$\epsilon = \frac{\lambda_{max}^2 - \lambda_{max}^{-2}}{2} \tag{10}$$

where $\lambda_{max} = a/a_0$ is the maximum equilibrium extension ratio in the elongation axis. Thus, the relationship between the equivalent point force F^* and the cell E-D follows,

$$\langle F^* \rangle = \mu b\left(\lambda_{max}^2 - \lambda_{max}^{-2}\right) \tag{11}$$

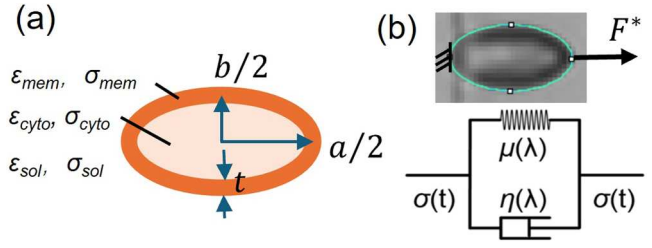

Fig. 1. Modeling of cell electromechanics associated with E-D. (a) single-shell ellipsoid model to evaluate (f_{CM}) based on the dielectric properties of cell and the measuring solution. (b) Kelvin-Voigt solid model to interpret the membrane elongation subjected to an applied electrical force.

2.2. Electro-deformation spectroscopy (EDS) experiment

Four healthy human blood samples were obtained, one through finger prick sampling (fb) with the authorization of the Institutional Review Board (IRB) at Florida Atlantic University, and three (bb#1 to bb#3) acquired from a local blood bank. The EDS measuring solution was prepared with 0.3 % (w/v) dextrose (Sigma Aldrich), and 8.5 % (w/v) sucrose (Sigma Aldrich) in deionized water. The conductivity of the solution was adjusted to 100 μS/cm by adding phosphate-buffered saline (Gibco® Life Technologies) at a volume ratio of 110 μL/15 mL and confirmed with a conductivity meter (Extech- EC500). Osmolality of the solution was 290 ± 10 mOsm/kg H_2O measured by an osmometer (Model 3300, Advanced Instruments Inc.), which was within the normal range of blood plasma, 275 to 295 mOsm/kg H_2O. The microchannel was primed using 30–40 μL measuring solution to keep wet before use. The whole blood specimen of 1 μL was diluted directly in 500 μL measuring solution. A 5 μL cell suspension was then added into the microfluidic device and gently pipetted into a uniform suspension. EDS measurements were performed at room temperature.

A schematic illustration of the EDS measurement principle is shown in Fig. 2a. The experimental setup consists of a function generator (SIGLENT SDG830), interdigitated microelectrodes, and a microscope camera for observation. AC excitations such as sinewaves are used to induce DEP that moves suspended cells towards the edge of electrodes and spontaneously, cell membranes are stretched by the electrical forces exerted on the cell membranes. Same design of microfluidic chip for the conventional E-D measurement and fatigue measurement [37,48] was used to perform the EDS. Briefly, the microfluidic device consists of a

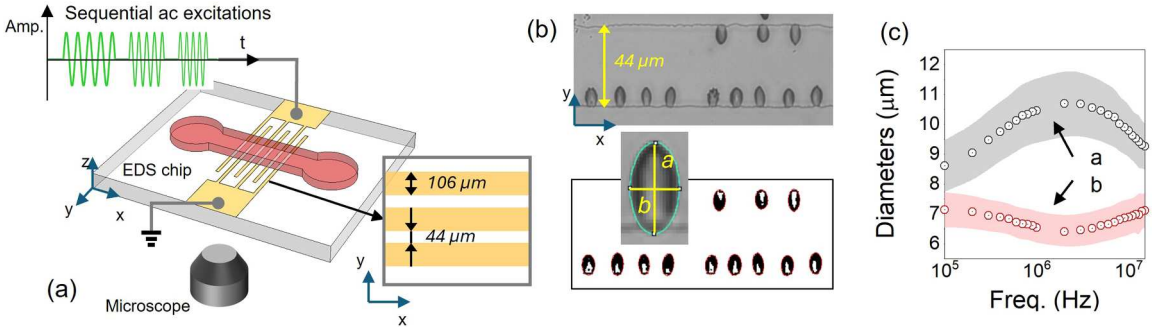

Fig. 2. Schematic of the EDS measurement principle. (a) A sequential sinewave is used to create electric fields of a fixed magnitude and varying electrical frequencies in the microfluidic chip. (b) Electro-deformation of cell membranes is analyzed, and diameters are measured through ellipse fitting of individual cells using ImageJ. (c) Representative electro-deformation of RBCs ($n = 163$) from sample fb shows inherent bio heterogeneity and frequency dependence. Symbols represent mean and shade represents the standard deviation.

pre-patterned indium tin oxide (ITO) electrode array (100 nm thick) coated on a 0.7 mm thick glass substrate, and a 75 μm deep polydimethylsiloxane (PDMS) channel. The gap and band width of the ITO electrodes used in this study were 44 μm and 106 μm, correspondingly. The microchannel has an inlet well and an outlet well of 3 mm and 1 mm for loading samples. The thin film electrode array created an asymmetric electric field, allowing EDS measurement of about fifty to one hundred cells in a single field of view under a 20× objective lens. A bandpass filter of 414/46 nm, near the peak of the hemoglobin absorption spectrum, was inserted in the optical path to optimize the image contrast and cell outlines.

It is natural that elliptical shapes will be fitted exactly matching the cell outline under E-D induced elongation (Fig. 2b). This can be done using standard image processing techniques. In this new method, the same cells within the field of view are measured for their E-D under a sequential of electrical frequencies, i.e., 15 MHz - 1 MHz with a decrement of 1 MHz and 900 kHz - 100 kHz with a decrement of 100 kHz. Sinewave signals of 1.5 V root mean square (V_{RMS}) were used to create the electric field. The nominal magnitude of field strength is 34 kV/m, following $E_n = V/\hat{g}$, where $\hat{g}$ is the gap of the coplanar electrodes. Cell response to ac excitations was nearly spontaneous. Cell membranes were fully stretched within a couple of seconds upon sinewave output from the function generator. Each frequency output was maintained briefly, ~2 s and the maximum deformation was recorded for analysis. The entire elongation time of EDS measurement was about 1 min, which did not cause significant morphological or mechanical changes in cell membranes as demonstrated in our prior fatigue experiment [37]. The major and minor diameters of individual cells show the inherent variations among cells within the same blood sample subjected to the ac electric fields. Such response is highly frequency dependent (Fig. 2c).

2.3. Decoupling of cell electromechanical characteristics

The elongation of cells induced by E-D excitation depends on the dielectric and mechanical characteristics of cells under testing. In this study, we demonstrate that the added dimension, electrical frequency, in the EDS measurement can be useful to decouple the entangled electrical and mechanical parameters through a combination of numerical analyses of the equivalent electrical force, F^* and the first order hyperelastic deformation of cell membranes as detailed below.

ImageJ [49] was used to identify single cells stretched at the electrode edges and tracked individually. Cells undergoing E-D exhibited uniaxial elongation, thus elliptical shapes will be fitted exactly matching the cell outline, with the major diameter, a in the elongation axis and the minor diameter, b perpendicular to that. Standard image processing techniques were used. Briefly, microscopic images were imported into ImageJ and converted into 8-bit format. Then, the application of the default thresholding algorithm identified the outline of single cells, in contrast to the white background. In the experiments, employing a bandpass filter close to the hemoglobin absorption spectrum peak significantly enhanced the precision of the outline identification. Note the diameter c in the z-axis, perpendicular to the view plane, was not measured but can be determined following volume conservation principle (CVP), which assumes the volume of a cell determined when it is at rest does not change during the EDS measurement. For a blood sample with known mean corpuscular volume (MCV) value, the initial value diameter in the 3rd axis when cells are at rest was assumed to be constant, c* and computed by,

$$c^* = MCV/\overline{SA} \tag{12}$$

where $\overline{SA}$ is the mean projected cell area prior to deformation, averaged from a population of cells per sample. Following the ellipsoid model, volume of each cell, V_{cell}, can be calculated based on the initial diameter d_0 of its undeformed shape in the x-y view and the initial value of c*,

$$V_{cell} = \frac{1}{6}\pi d_0^2 c^* \tag{13}$$

When cell is deformed, the third axis c is computed following CVP and the ellipsoid model. To find the best fit parameters for cell electrical and mechanical properties, i.e., relative permittivity of cell membrane, ε_{mem}, cytoplasm conductivity, σ_{cyto}, and membrane shear modulus, μ, the objective function is defined as,

$$\begin{aligned} &Given\ x = \langle \varepsilon_{mem},\ \sigma_{cyto},\ \mu \rangle \\ &Minimize\ Q(x) = \sum_{i=1}^{n} \left[Re\left(f_{CM}^{theo}\right)_i - Re\left(f_{CM}^{exp}\right)_i \right]^2 \\ &\quad such\ that \\ &\quad 0.7 - R^2 \le 0 \\ &\quad 0.1 \le \varepsilon_{mem} \le 30 \\ &\quad 0.1 \le \sigma_{cyto} \le 3\frac{S}{m} \\ &\quad 0.1 \le \mu \le 30\frac{\mu N}{m} \end{aligned} \tag{14}$$

where i is the index to frequency, $Re\left(f_{CM}^{theo}\right)$ is the theoretical CM factor determined from Eq. (4), and $Re\left(f_{CM}^{exp}\right)$ is the experimental CM factor determined from Eqs. (7) & (11). The nonlinear constraint was applied to the optimization problem to ensure the quality of the fit R^2 is no less than 0.7, using the coefficient of determination,

$$R^2 = 1 - \frac{Q}{\sum_{i=1}^{n}\left(Re\left(f_{CM}^{exp}\right)_i - \overline{Re\left(f_{CM}^{theo}\right)}\right)^2} \tag{15}$$

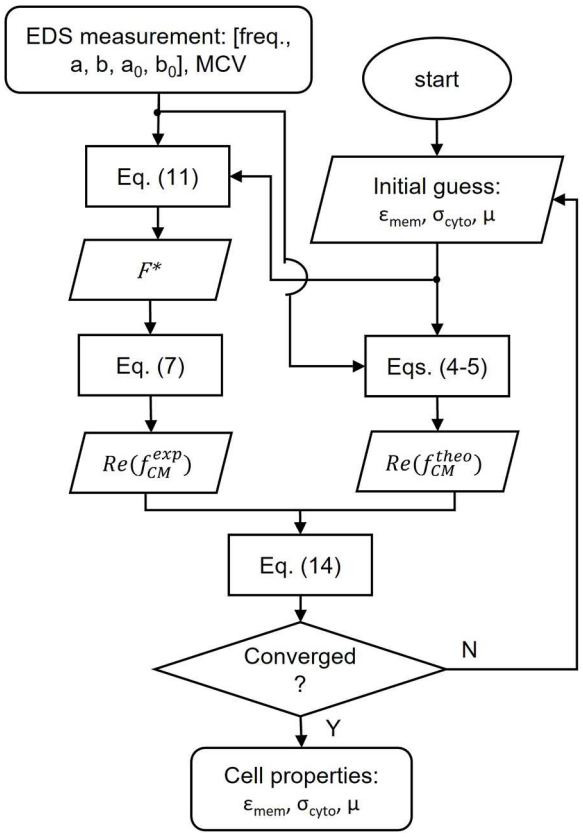

Fig. 3. Flow chart of the optimization process for data fitting.

where $\overline{Re\left(f_{CM}^{theo}\right)} = \sum_{i=1}^{n} \left(Re\left(f_{CM}^{exp}\right)_i\right)/n$.

Solving the above optimization problem will decouple the electrical and mechanical characteristics of the EDS measurement. A custom MATLAB script was implemented to solve the optimization problem with the built-in minimization solver, *fmincon*, following the flow chart of the data fitting (Fig. 3). Two assumptions on the non-dominant cell dielectric parameters were made. Firstly, the relative permittivity of cell interior ε_{cyto} has negligible effect on the $Re(f_{CM})$ for frequencies less than 15 MHz theoretically. This was further confirmed by MyDEP [50] prediction using single-shell spheroid model with ε_{cyto} in a wide range of 30–80. Secondly, the plasma membranes have very high electrical resistance; correspondingly, membrane conductivity, σ_{mem} has a negligible effect on the $Re(f_{CM})$ for frequencies higher than 500 kHz. This was further confirmed by MyDEP prediction using single-shell spheroid model with $\sigma_{mem} = [1 \times 10^{-7}, 1 \times 10^{-5}]$ S/m. Therefore, for simplicity, standard values of cell interior permittivity, ε_{cyto}= 59 and membrane conductivity, σ_{mem}= 1×10^{-6} S/m [51] were used in the data fitting algorithm.

2.4. Statistical analysis

RBCs were individually tracked across frequencies for EDS analysis. Statistical analysis was performed with OriginPro2020 (OriginLab, Northampton, MA). All data were expressed as mean ± SD, unless stated otherwise. Normality of the data was assessed using the Kolmogorov-Smirnov test. Kruskal-Wallis test was used to evaluate the difference among the population of the four normal blood samples. P-values of 0.05 or less were considered significant.

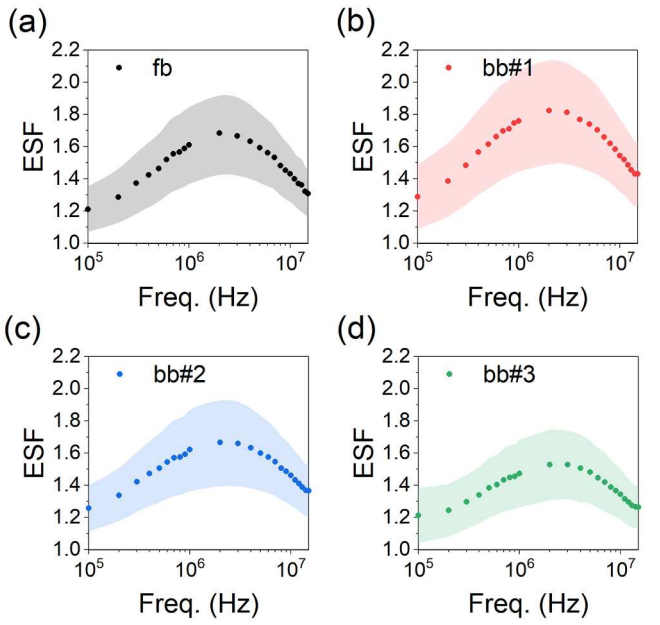

Fig. 4. Population mean-based cell elongation analysis shows strong frequency-dependence in E-D response among all the samples under testing (a) fb, and (b-d) for sample bb#1–3, respectively. Shade shows the standard deviation.

Table 1
Population-mean based analysis and biophysical characteristics of the blood samples.

Sample#	MCV (fL)	c* (μm)	[a]d_0 (μm)	ESF @2MHz	[b]ESF @2MHz	[c]K-S test p-value
fb	85	2.7	7.8 ± 0.8	1.68 ± 0.25	1.67	0.8
bb#1	94	3.0	7.7 ± 0.6	1.82 ± 0.33	1.80	0.3
bb#2	91	2.7	8.1 ± 0.7	1.67 ± 0.27	1.67	0.2
bb#3	89	2.7	7.9 ± 0.6	1.53 ± 0.22	1.54	0.03

[a] Equivalent diameter of undeformed cells from image analysis. Values of d_0 were averaged based on a population of RBCs for fb: n = 163, bb#1: n = 95, bb#2: n = 117, and bb#3: n = 183.
[b] Median value of the ESF.
[c] K-S test: Kolmogorov-Smirnov test of normality.

3. Results

3.1. Cell elongation analysis

Level of elongation was quantified by the elliptical shape factor (ESF), defined as the ratio of the major and minor diameters of the ellipse, ESF = a/b. RBCs from all the four blood samples showed strong frequency-dependence response subjected to the ac electric fields (Fig. 4). It was also noted that sample fb and bb#2 shared similar response, bb#1 showed the highest elongation while bb#3 had the least elongation. Unanimously, the maximum elongation occurred around 2 MHz, although the exact elongation level differed markedly among the samples. This comparable pattern is likely to be attributed to the healthy state of the tested blood samples. In addition, the intrasample variation was obvious for all the blood samples, indicating the inherent bioheterogeneity.

The detailed descriptive analysis and biophysical characteristics of the four blood samples fb, bb#1–3 were summarized in Table 1. The parameters of interest included the MCV, cell thickness (c*), equivalent

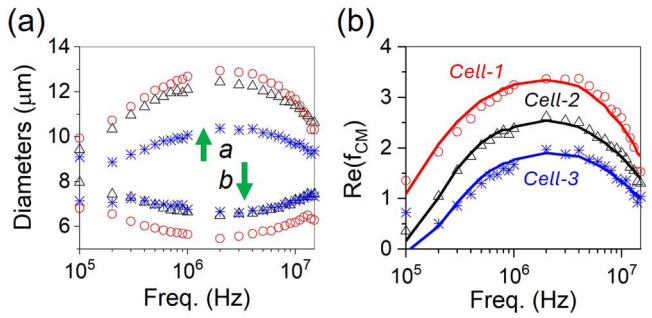

Fig. 5. Representative single-cell EDS analysis. (a) Diameters of three individually tracked cells from sample bb#3 showed varied degree of elongation. (b) Corresponding theoretical *Re*(f_{CM}) values (curves) and experimental measurements (symbols) for the three cells shown in (a). Each symbol type represents a different cell. Electromechanical decoupling results for cell-1 (red circles): ε_{mem} = 2.8, σ_{cyto} = 0.60 S/m, and μ = 2.7 μN/m; cell-2 (black triangles): ε_{mem} = 5.9, σ_{cyto} = 0.89 S/m, and μ = 2.0 μN/m; and cell-3 (blue stars): ε_{mem} = 2.1, σ_{cyto} = 0.42 S/m, and μ = 3.1 μN/m.

diameter (d_0) of the undeformed cells, and the ESF values assessed at 2 MHz. Cell thickness was calculated using Eq. (12). Elongation levels of all samples except bb#3 exhibited normal distribution. Median ESF values ranged from 1.54 to 1.80. No obvious correlation was found between the elongation level and the intrinsic biophysical characteristics such as cell volume and diameters. For example, blood sample bb#3 has moderate cell volume (89 fL) and moderate diameter (7.9 μm), but its elongation level is the lowest among all samples.

3.2. Single-cell EDS analysis

Fig. 5a depicts the single-cell EDS of three representative cells from sample bb#3 that were traced individually across frequencies. There were noticeable differences in cell size as well as the level of elongation observed. When analyzing the EDS on a single-cell basis, it's evident that there were significant differences in dielectric and mechanical attributes amongst the cells. The cell denoted by blue stars (cell-3), which exhibited the least elongation, had the lowest *Re*(f_{CM}) and highest membrane shear modulus μ (3.1 μN/m). The other two cells denoted by triangles and circles had relatively greater elongations across frequencies and lower shear modulus of elasticity, being 2.7 μN/m and 2.0 μN/m, respectively. Nonetheless, the degree of elongation does not always correlate with membrane deformability (ESF value) or membrane shear modulus, because the dielectric and mechanical characteristics become complexly interwoven during cell E-D as described by the relevant mathematical models of cell electromechanics.

Table 2
Averaged single-cell EDS measurements.

Sample#	[a]ε_{mem}	σ_{cyto} (S/m)	μ (μN/m)	[b]C_{mem} (mF/m^2)
fb	3.6 ± 1.9	0.57 ± 0.24	2.3 ± 0.6	7.2
bb#1	5.2 ± 2.4	0.77 ± 0.34	2.2 ± 0.7	10.3
bb#2	5.8 ± 3.7	0.81 ± 0.39	2.7 ± 0.8	11.5
bb#3	3.6 ± 2.7	0.47 ± 0.20	2.8 ± 0.6	7.2
Standard values[c]	4.4 – 9.5	0.31 – 1.44	2.4 – 5.5	7 - 14.3
	Refs. [51, 52]	Refs. [51–53]	Refs. [54, 55]	Refs. [56–58]

[a] All values are mean ± SD. (fb: n = 158; bb#1: n = 90; bb#2: n = 109; bb#3: n = 166).
[b] C_{mem} is calculated based on the average single-cell membrane permittivity and membrane thickness of 4.5 nm based on parallel plate capacitor.
[c] Literature values were obtained using both classical population-based approaches such as dielectric and impedance spectroscopy and single-cell techniques such as micropipette aspiration, optical tweezers, dielectrophoresis and electrorotation.

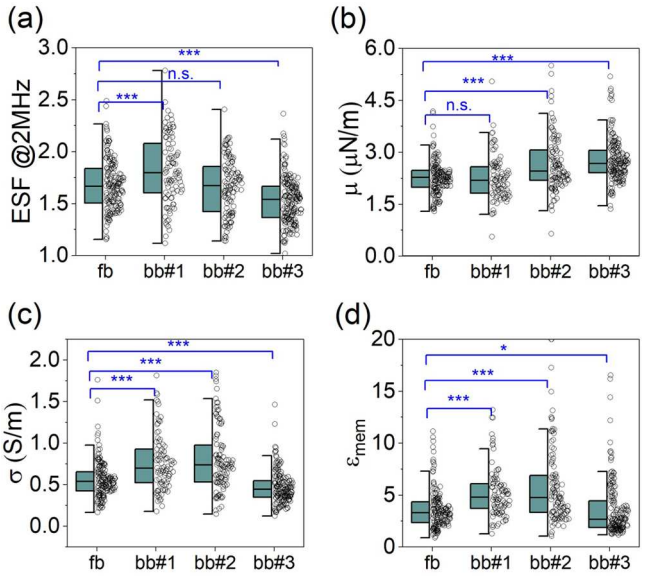

Fig. 6. Individual variability among the four blood samples under testing evaluated by various parameters: (a) ESF value at the frequency of 2 MHz, (b) membrane shear modulus, (c) electrical conductivity of cytoplasm, and (d) relative permittivity of cell membranes. Each symbol represents a single cell measurement. Box chart shows median value and 25 and 75 percent range of measurements. n.s. – not significant. * $p < 0.05$. *** $p < 0.001$. Populations are significantly different ($p < 0.001$) based on each parameter (not shown in the figure).

Having established that the solution to the optimization problem as described in Eq. (14) is capable of deriving electrical and mechanical cell properties from EDS experiments, we subsequently analyzed individually tracked cells in all the blood samples. To confirm the validity of the single-cell EDS approach, Table 2 compares the values of the membrane shear modulus μ, relative permittivity of cell membrane ε_{mem}, and cytoplasm conductivity σ_{cyto} per each blood sample obtained from current study to the standard values in the literature. We found that the mechanical property, membrane shear modulus of elasticity fell within relatively narrow range, being 2.2 – 2.8 μN/m. This is probably indicative of the integrity of healthy RBC membranes across all blood samples. The cytoplasm conductivity varied from 0.47 – 0.81 S/m, which may reflect the differences in cellular water content, hemoglobin concentration, and ionic strength in different blood samples. The relative permittivity of cell membranes ranged from 3.6 – 5.8, which shows the individual difference in capacitance or polarization. Nonetheless, these values align reasonably well with the standard values for normal human RBCs. It is noted that the standard values for cell membrane dielectric properties span a wide range, including a relative permittivity of 4.4 - 9.5, membrane capacitance of 7 - 14.3 mF/m^2, and cytoplasm conductivity of 0.31 - 1.44 S/m. The standard values for membrane shear modulus also show a wide range between 2.4 and 5.5 μN/m. These broader ranges of standard values may result from different methods and testing conditions reported in the literature.

The population of the four blood samples was significantly different ($p < 0.001$), according to the Kruskal-Wallis ANOVA test detailed in the figure (Fig. 6). It is noted that such difference can be identified using each of the parameters from EDS analysis, including ESF, membrane shear modulus, membrane permittivity and cytoplasm conductivity. Among the four samples, bb#2 and #3 have higher shear moduli, indicating the RBCs from these two samples are more rigid than the other two blood samples (Fig. 6b). Samples bb#1 and #2 have significantly higher cytoplasm conductivity than the other two samples (Fig. 6c), indicating the cellular interior has lower resistance to the

electric currents, which could link to the contributing factors such as intracellular composition, hemoglobin concentration, and ions, as discussed in detail in literature [53].

Importantly, single-cell EDS analysis reveals individual variability and sample heterogeneity that was not captured by elongation observations, e.g., ESF value. While morphology-based analysis aids in assessing cell deformability, a commonly used assessment in literature, it lacks the precision to measure membrane elasticity or to detect difference among normal blood samples. For instance, samples fb and bb#2 showed comparable elongation levels but had significantly different membrane elasticity ($p < 0.001$, Fig. 6b), which could largely attribute to the variations in cytoplasm conductivity ($p < 0.001$, Fig. 6c) and membrane permittivity ($p < 0.001$, Fig. 6d). Conversely, samples with similar membrane shear modulus such as between fb and bb#1, exhibited significantly different elongation ($p < 0.001$, Fig. 6a), which are largely due to their different cytoplasm conductivity ($p < 0.001$, Fig. 6c) and membrane permittivity ($p < 0.001$, Fig. 6d). From the single-cell EDS analysis, we can infer that elongation is not dependent on membrane elasticity alone. Conversely, given samples of similar membrane elasticity, their deformation may be different due to variations in cellular electrical properties. These results aligned with the dielectric model of the cell discussed in the cell electromechanics modeling section.

4. Discussion

4.1. Electrical conductivity of blood plasma and intracellular content

The electrical conductivity of human blood plasma is much higher at 1.48 S/m [59] than the measuring solution, 0.01 S/m. Although plasma presence in whole blood can raise the overall medium conductivity, its impact is minimal in this study because of the thousandfold dilution. Thus, utilizing the measuring solution conductivity for EDS analysis is reasonably justified. The literature reports a broad range of cytoplasm electrical conductivity, but there is an agreement that physiological conductivity at room temperature falls between a relatively narrow range of 0.31 S/m - 0.56 S/m [51,53], which overlaps with the median figures of the samples in current study, 0.45 – 0.74 S/m. The small discrepancy may be due to different measurement techniques compared with standard electrical methods like dielectric and impedance spectroscopy or ac electrokinetic methods such as dielectrophoresis and electrorotation.

4.2. Electrical force calibration and strain measurements

The EDS method evaluates cell deformation in ac electric fields where measurement precision is closely linked to calibration of the electrical forces. In our analysis, several factors must be considered to ensure accurate interpretation of the data. One critical aspect is the approximation of the electrical force that is responsible for cell elongation. In the current approach, an equivalent point force was approximated and assumed act at the far end point of cells undergoing electrodeformation. Compared to the more rigorous MTS method, the location of the equivalent point force may lead to an underestimation of the force magnitude because the electric field strength diminishes as the distance from the electrode edge increases. Similar to other ac electrokinetic methods, where two dimensional (2D) images of cell movement (in the context of dielectrophoresis and electrorotation), cell elongation (electro-deformation) for EDS analysis are seen in the x-y plane. However, the true elongation of cells occurs at a small angle relative to this plane due to the influence of radial electric field lines. Consequently, the measured elongation in the x-y plane tends to underestimate the actual deformation experienced by the cells. This goes on to the strain, $\epsilon \propto \lambda_{max}^2$. Additionally, because the electrical force exerted on the cells is generally proportional to their volume, $F \propto abc$, the calibrated force might be slightly lower than the true force applied. Therefore, the combined effects of underestimating both the electrical force and the actual elongation suggest that the shear modulus of elasticity might be slightly overestimated in this context.

4.3. Restrictions of single-cell EDS

The primary restriction of the EDS measurements is that cells must exhibit measurable deformation (or strain). For cells with extremely high modulus of elasticity, a very high electrical force would be needed. This can be achieved from two aspects. Firstly, once can increase the ac field magnitude as $\boldsymbol{F} \propto \nabla \boldsymbol{E}_{rms}^2$ by increasing the voltage level or decreasing the electrode gap. However, one should note the influences from increasing voltage levels. One possible influence is Joule heating [60], which may cause variations in material properties and goes on to the cell properties. Another potential influence is the dielectric membrane breakdown [61]. It happens if the total membrane potential difference exceeds the breakdown voltage at a given critical electric field strength of E_c, as $V_c = 1.5E_c \cdot r \cdot cos\alpha \pm V_m$, where r is the radius of the cell, E_c is the critical electric field, and V_m is the resting membrane potential difference [62]. At room temperature, the breakdown voltage for plasma membrane is around 1 V and it increases as the temperature drops. Given the resting transmembrane potential difference of RBCs, V_m = -90 mV [63], the applied electric field, 34 kV/m used in current study was far below the critical field strength 152 kV/m for a 8 μm diameter sized cell. Secondly, one can modify the experimental conditions to improve the difference in the polarizability between the cells under measurements and the testing solution. This is reflected in the factor of f_{CM} where the electrical force is directly proportional to its real value. For many biological cells, a lower conductivity solution would be used for a favorable $Re(f_{CM})$ to generate electrical force using low electric field strength.

Another restriction of the EDS measurements is that cellular response to the applied ac electric fields must be frequency dependent. This is inherent to the factor of f_{CM}, which is a strong function of electrical frequency. The EDS measurements should be carried out within a frequency range that ensures $Re(f_{CM})$ is positive. Therefore, the frequency range for EDS measurements should be adjusted accordingly based on the cell type. Since the selection of the frequencies align with the conditions for positive DEP, one can use the tools such as myDEP [50] to predict the behavior of cells of interest and design the EDS experiment accordingly.

5. Conclusions

This paper demonstrated a new single-cell approach for simultaneous characterization of electrical and mechanical properties of cells, including membrane permittivity, cytoplasm conductivity, and membrane shear modulus. Noted advantages of this approach include the simplicity in operation, time efficiency and moderate throughput. The testing protocol developed for current study can be used to measure whole blood directly with minimal sample preparation. Each EDS experiment takes about 1 min, and 50 −100 single cells can be measured per experiment without optimal design of the electrodes. Although the number of cells in the field of view can be much more than this range, the RBC “pearl chain” formation [64] along the electric field lines due to particle polarization makes it challenging to track individual cells across frequencies, hence, the actual number of cells available for single-cell EDS analysis is less. Ways to improve the throughput include increasing the number of interdigitated electrodes, such that more cells per field can be tested, and cell concentration can be optimized to allow more uniformly distributed cells with cell interactions minimized. The developed protocol, mathematical model of cell electromechanics, and the method for analysis can be readily translated to measure RBCs in other conditions or cell types of similar structure. The framework also

lays the foundation for further refinement so that the EDS technique can be extended to other biological cells in general and for further development into a standardized tool for single cell biomechanical and electrical characterizations.

Data availability

Data will be made available on request.

Abbreviations

EDS, electro-deformation spectroscopy; E-D, electro-deformation; AC, alternating current; DEP, dielectrophoresis; RBC, red blood cell; f_{CM}, Clausius Mossotti factor; MCV, mean corpuscular volume; ITO, indium tin oxide.

CRediT authorship contribution statement

E Du: Writing – review & editing, Writing – original draft, Visualization, Validation, Supervision, Software, Resources, Project administration, Methodology, Investigation, Funding acquisition, Formal analysis, Data curation, Conceptualization. **Hongyuan Xu:** Methodology, Investigation, Formal analysis, Data curation. **Liliana Ponkratova:** Investigation, Formal analysis, Data curation.

Declaration of competing interest

The authors declare that they have no known competing financial interests or personal relationships that could have appeared to influence the work reported in this paper.

Acknowledgement

This material is based upon work supported by the National Science Foundation under Grant No. 1941655 and No. 2032730. Author E.D. acknowledges the support of the National Institutes of Health under Grant No. R01AI169648, and the I-HEALTH and I-SENSE pilot grants from Florida Atlantic University.

References

[1] D. Miklavčič, N. Pavšelj, F.X. Hart, Electric properties of tissues. Wiley Encyclopedia of Biomedical Engineering, Wiley, 2006.
[2] K.R. Foster, H.P. Schwan, Dielectric properties of tissues, CRC handbook of biological effects of electromagnetic fields (2019) 27–96.
[3] M.A. Meyers, P.Y. Chen, A.Y.M. Lin, Y. Seki, Biological materials: structure and mechanical properties, Prog. Mater. Sci. 53 (1) (2008) 1–206.
[4] T.M. Evers, L.J. Holt, S. Alberti, A. Mashaghi, Reciprocal regulation of cellular mechanics and metabolism, Nat. Metab. 3 (4) (2021) 456–468.
[5] S. Suresh, J. Spatz, J.P. Mills, A. Micoulet, M. Dao, C. Lim, M. Beil, T. Seufferlein, Connections between single-cell biomechanics and human disease states: gastrointestinal cancer and malaria, Acta Biomater. 1 (1) (2005) 15–30.
[6] G.Y. Lee, C.T. Lim, Biomechanics approaches to studying human diseases, Trends Biotechnol. 25 (3) (2007) 111–118.
[7] S. Suresh, Biomechanics and biophysics of cancer cells, Acta Biomater. 3 (4) (2007) 413–438.
[8] S. Kerdegari, P. Canepa, D. Odino, R. Oropesa-Nuñez, A. Relini, O. Cavalleri, C. Canale, Insights in cell biomechanics through atomic force microscopy, Materials 16 (8) (2023) 2980.
[9] M. Nötzel, G. Rosso, S. Möllmert, A. Seifert, R. Schlüßler, K. Kim, A. Hermann, J. Guck, Axonal transport, phase-separated compartments, and neuron mechanics-a new approach to investigate neurodegenerative diseases, Front. Cell. Neurosci. 12 (2018) 358.
[10] D. Discher, C. Dong, J.J. Fredberg, F. Guilak, D. Ingber, P. Janmey, R.D. Kamm, G. W. Schmid-Schönbein, S. Weinbaum, Biomechanics: cell research and applications for the next decade, Ann. Biomed. Eng. 37 (2009) 847–859.
[11] M. Mozneb, E. Mirtaheri, A.O. Sanabria, C.Z. Li, Bioelectronic properties of DNA, protein, cells and their applications for diagnostic medical devices, Biosens. Bioelectron. 167 (2020) 112441.
[12] T. Chalklen, Q. Jing, S. Kar-Narayan, Biosensors based on mechanical and electrical detection techniques, Sensors 20 (19) (2020) 5605.
[13] D. Spencer, H. Morgan, High-speed single-cell dielectric spectroscopy, ACS Sens. 5 (2) (2020) 423–430.
[14] D. Dieujuste, Y. Qiang, E. Du, A portable impedance microflow cytometer for measuring cellular response to hypoxia, Biotechnol. Bioeng. 118 (10) (2021) 4041–4051.
[15] J.C. Chien, A. Ameri, E.C. Yeh, A.N. Killilea, M. Anwar, A.M. Niknejad, A high-throughput flow cytometry-on-a-CMOS platform for single-cell dielectric spectroscopy at microwave frequencies, Lab Chip 18 (14) (2018) 2065–2076.
[16] E.A. Henslee, Dielectrophoresis in cell characterization, Electrophoresis 41 (21–22) (2020) 1915–1930.
[17] G. De Gasperis, X. Wang, J. Yang, F.F. Becker, P.R. Gascoyne, Automated electrorotation: dielectric characterization of living cells by real-time motion estimation, Meas. Sci. Technol. 9 (3) (1998) 518.
[18] L. Huang, Q. Fang, Electrical properties characterization of single yeast cells by dielectrophoretic motion and electro-rotation, Biomed. Microdevices 23 (1) (2021) 11.
[19] H. Morgan, T. Sun, D. Holmes, S. Gawad, N.G. Green, Single cell dielectric spectroscopy, J. Phys. D Appl. Phys. 40 (1) (2006) 61.
[20] K. Heileman, J. Daoud, M. Tabrizian, Dielectric spectroscopy as a viable biosensing tool for cell and tissue characterization and analysis, Biosens. Bioelectron. 49 (2013) 348–359.
[21] N. Nasir, M. Al Ahmad, Cells electrical characterization: dielectric properties, mixture, and modeling theories, J. Eng. 2020 (2020) 1–17.
[22] F. Basoli, S.M. Giannitelli, M. Gori, P. Mozetic, A. Bonfanti, M. Trombetta, A. Rainer, Biomechanical characterization at the cell scale: present and prospects, Front. Physiol. 9 (2018) 1449.
[23] G. Pesce, P.H. Jones, O.M. Maragò, G. Volpe, Optical tweezers: theory and practice, Eur. Phys. J. Plus 135 (2020) 1–38.
[24] M. Diez-Silva, M. Dao, J. Han, C.T. Lim, S. Suresh, Shape and biomechanical characteristics of human red blood cells in health and disease, MRS Bull. 35 (5) (2010) 382–388.
[25] G. Runel, N. Lopez-Ramirez, J. Chlasta, I. Masse, Biomechanical properties of cancer cells, Cells 10 (4) (2021) 887.
[26] Y. Nematbakhsh, C.T. Lim, Cell biomechanics and its applications in human disease diagnosis, Acta Mech. Sin. 31 (2015) 268–273.
[27] V. Sheikhhassani, T.M. Evers, S. Lamba, F. Shokri, A. Mashaghi, Single cell force spectroscopy of erythrocytes at physiological and febrile temperatures reveals mechano-modulatory effects of atorvastatin, Soft Matter 18 (11) (2022) 2143–2148.
[28] J. Teixeira, F.C. Moreira, J. Oliveira, V. Rocha, P.A. Jorge, T. Ferreira, N.A. Silva, Autonomous and intelligent optical tweezers for improving the reliability and throughput of single particle analysis, Meas. Sci. Technol. 35 (2) (2023) 025208.
[29] Y. Hao, S. Cheng, Y. Tanaka, Y. Hosokawa, Y. Yalikun, M. Li, Mechanical properties of single cells: measurement methods and applications, Biotechnol. Adv. 45 (2020) 107648.
[30] M. Gharooni, A. Alikhani, H. Moghtaderi, H. Abiri, A. Mashaghi, F. Abbasvandi, M. A. Khayamian, Z.S. Miripour, A. Zandi, M. Abdolahad, Bioelectronics of the cellular cytoskeleton: monitoring cytoskeletal conductance variation for sensing drug resistance, ACS Sens. 4 (2) (2018) 353–362.
[31] J. Chen, Y. Zheng, Q. Tan, Y.L. Zhang, J. Li, W.R. Geddie, M.A. Jewett, Y. Sun, A microfluidic device for simultaneous electrical and mechanical measurements on single cells, Biomicrofluidics 5 (1) (2011).
[32] J. Chen, M. Abdelgawad, L. Yu, N. Shakiba, W.Y. Chien, Z. Lu, W.R. Geddie, M. A. Jewett, Y. Sun, Electrodeformation for single cell mechanical characterization, J. Micromech. Microeng. 21 (5) (2011) 054012.
[33] Y. Teng, K. Zhu, C. Xiong, J. Huang, Electrodeformation-based biomechanical chip for quantifying global viscoelasticity of cancer cells regulated by cell cycle, Anal. Chem. 90 (14) (2018) 8370–8378.
[34] S. Moazzeni, Y. Demiryurek, M. Yu, D.I. Shreiber, J.D. Zahn, J.W. Shan, R.A. Foty, L. Liu, H. Lin, Single-cell mechanical analysis and tension quantification via electrodeformation relaxation, Phys. Rev. E 103 (3) (2021) 032409.
[35] L.A. MacQueen, M.D. Buschmann, M.R. Wertheimer, Mechanical properties of mammalian cells in suspension measured by electro-deformation, J. Micromech. Microeng. 20 (6) (2010) 065007.
[36] P. Peterlin, Frequency-dependent electrodeformation of giant phospholipid vesicles in AC electric field, J. Biol. Phys. 36 (2010) 339–354.
[37] Y. Qiang, J. Liu, M. Dao, S. Suresh, E. Du, Mechanical fatigue of human red blood cells, Proc. Natl. Acad. Sci. 116 (40) (2019) 19828–19834.
[38] Y. Qiang, J. Liu, M. Dao, E. Du, *In vitro* assay for single-cell characterization of impaired deformability in red blood cells under recurrent episodes of hypoxia, Lab Chip 21 (18) (2021) 3458–3470.
[39] N.G. Green, H. Morgan, Dielectrophoretic investigations of sub-micrometre latex spheres, J. Phys. D Appl. Phys. 30 (18) (1997) 2626.
[40] S. Kumar, P.J. Hesketh, Interpretation of ac dielectrophoretic behavior of tin oxide nanobelts using Maxwell stress tensor approach modeling, Sens. Actuators B Chem. 161 (1) (2012) 1198–1208.
[41] H. Morgan, N.G. Green, AC Electrokinetics, Research Studies Press, 2003.
[42] M. Castellarnau, A. Errachid, C. Madrid, A. Juarez, J. Samitier, Dielectrophoresis as a tool to characterize and differentiate isogenic mutants of Escherichia coli, Biophys. J. 91 (10) (2006) 3937–3945.
[43] L. Zheng, J.P. Brody, P.J. Burke, Electronic manipulation of DNA, proteins, and nanoparticles for potential circuit assembly, Biosens. Bioelectron. 20 (3) (2004) 606–619.
[44] Y. Qiang, J. Liu, F. Yang, D. Dieujuste, E. Du, Modeling erythrocyte electrodeformation in response to amplitude modulated electric waveforms, Sci. Rep. 8 (1) (2018) 10224.
[45] E. Evans, R. Waugh, Osmotic correction to elastic area compressibility measurements on red cell membrane, Biophys. J. 20 (3) (1977) 307–313.

[46] R.M. Hochmuth, P. Worthy, E.A. Evans, Red cell extensional recovery and the determination of membrane viscosity, Biophys. J. 26 (1) (1979) 101–114.
[47] E.A. Evans, R.M. Hochmuth, A solid-liquid composite model of the red cell membrane, J. Membr. Biol. 30 (1) (1976) 351–362.
[48] D. Dieujuste, A.K. Alamouti, H. Xu, E. Du, Amplitude-modulated electrodeformation to evaluate mechanical fatigue of biological cells, JoVE (J. Vis. Exp.) 200 (2023) e65897.
[49] T.J. Collins, ImageJ for microscopy, Biotechniques 43 (S1) (2007) S25–S30.
[50] J. Cottet, O. Fabregue, C. Berger, F. Buret, P. Renaud, M. Frénéa-Robin, MyDEP: a new computational tool for dielectric modeling of particles and cells, Biophys. J. 116 (1) (2019) 12–18.
[51] P. Gascoyne, C. Mahidol, M. Ruchirawat, J. Satayavivad, P. Watcharasit, F. F. Becker, Microsample preparation by dielectrophoresis: isolation of malaria, Lab Chip 2 (2) (2002) 70–75.
[52] A. Di Biasio, C. Cametti, Effect of the shape of human erythrocytes on the evaluation of the passive electrical properties of the cell membrane, Bioelectrochemistry 65 (2) (2005) 163–169.
[53] C.J. Sudsiri, R.J. Ritchie, Energy absorption of human red blood cells and conductivity of the cytoplasm influenced by temperature, Biophys. Chem. 273 (2021) 106578.
[54] G. Lenormand, S. Hénon, A. Richert, J. Siméon, F. Gallet, Direct measurement of the area expansion and shear moduli of the human red blood cell membrane skeleton, Biophys. J. 81 (1) (2001) 43–56.
[55] Y.P. Liu, C. Li, K.K. Liu, A.C. Lai, The deformation of an erythrocyte under the radiation pressure by optical stretch, (2006).
[56] J.Z. Bao, C.C. Davis, R. Schmukler, Frequency domain impedance measurements of erythrocytes. Constant phase angle impedance characteristics and a phase transition, Biophys. J. 61 (5) (1992) 1427–1434.
[57] R. Lisin, B.Z. Ginzburg, M. Schlesinger, Y. Feldman, Time domain dielectric spectroscopy study of human cells. I. Erythrocytes and ghosts, Biochim. Biophys. Acta (BBA)-Biomembr. 1280 (1) (1996) 34–40.
[58] F. Bordi, C. Cametti, T. Gili, Dielectric spectroscopy of erythrocyte cell suspensions. A comparison between Looyenga and Maxwell–Wagner–Hanai effective medium theory formulations, J. Non-Cryst. Solids 305 (1–3) (2002) 278–284.
[59] C.J. Sudsiri, R.J. Ritchie, Influence of Na+ disorder on cytoplasmic conductivity and cellular electromagnetic (EM) energy absorption of human erythrocytes (PONE-D-21-36089), PLoS ONE 18 (2) (2023) e0277044.
[60] X. Xuan, Joule heating in electrokinetic flow, Electrophoresis 29 (1) (2008) 33–43.
[61] J. Akinlaja, F. Sachs, The breakdown of cell membranes by electrical and mechanical stress, Biophys. J. 75 (1) (1998) 247–254.
[62] U. Zimmermann, G. Neil, The effect of high intensity electric field pulses on eukaryotic cell membranes: fundamentals and applications, in: Electromanipulation of Cells, 1, CRC Press, 1996, p. 106.
[63] M.M. Balach, C.H. Casale, A.N. Campetelli, Erythrocyte plasma membrane potential: past and current methods for its measurement, Biophys. Rev. 11 (6) (2019) 995–1005.
[64] H. Schwan, Dielectrophoresis and rotation of cells. Electroporation and Electrofusion in Cell Biology, Springer, 1989, pp. 3–21.